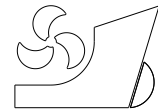


*Ozren Bukovac
Vladimir Medica
Vedran Mrzljak*



ISSN 1333-1124
eISSN 1849-1391

STEADY STATE PERFORMANCES ANALYSIS OF MODERN MARINE TWO-STROKE LOW SPEED DIESEL ENGINE USING MLP NEURAL NETWORK MODEL

UDC 629.54:621.436.13:519.6

Original scientific paper

Summary

Compared to the other marine engines for ship propulsion, turbocharged two-stroke low speed diesel engines have advantages due to their high efficiency and reliability. Modern low speed "intelligent" marine diesel engines have a flexibility in its operation due to the variable fuel injection strategy and management of the exhaust valve drive. This paper carried out verified zerodimensional numerical simulations which have been used for MLP (Multilayer Perceptron) neural network predictions of marine two-stroke low speed diesel engine steady state performances. The developed MLP neural network was used for marine engine optimized operation control. The paper presents an example of achieving lowest specific fuel consumption and for minimization of the cylinder process highest temperature for reducing NO_x emission. Also, the developed neural network was used to achieve optimal exhaust gases heat flow for utilization. The obtained data maps give insight into the optimal working areas of simulated marine diesel engine, depending on the selected start of the fuel injection (*SOI*) and the time of the exhaust valve opening (*EVO*).

Key words: Marine two-stroke diesel engine; MLP neural network; Numerical simulation; Utilization; Start of fuel injection; Time of exhaust valve open;

1. Introduction

Two-stroke diesel engines are the main component of ship propulsion. They are applied for propulsion of different ship types and classes due to their low price (regarding other propulsion machines), reliability, high efficiency and their very simple maintenance and servicing [1].

Turbocharging provides an increase in engine power and a modest reduction of specific fuel consumption [2]. Turbocharging causes an increase of medium effective pressure and maximum temperature of the in-cylinder process. This has an influence on the strain of engine components (as a result of differing thermal expansions) and also on the emissions of pollutants [3].

The diesel engine, as the main ship propulsion device, has to maintain very high reliability of its operation, even with the allowed degradation of performance when a failure occurs [4]. Precisely for this reason it is necessary to continuously monitor all the engine major operating parameters. Intelligent control system of the engine must have access to all diagnostic data and be able to adapt the engine to the optimal mode for desired operation [5].

In this paper, the main observed points were the engine steady states, although the numerical simulation model was not limited to steady state engine operation only. Standard engine simulations rarely include an analysis of engine transients and engine behaviour in exchanged working conditions. Simulation models based on neural networks in marine propulsion systems can achieve a number of objectives, such as the optimization of the propulsion system by changing the configuration or customizing the engine control settings [6], [7].

2. Engine specifications

Two-stroke low speed marine diesel engine 6S50MC MAN B&W, whose data were used for numerical simulations, Table 1, is originally not designed for variable settings in fuel injection and exhaust valve opening. This can be done with the same manufacturer modified engine design, which has a new designation MCE for "intelligent" engine variant (electronically controlled electro-hydraulic drives for exhaust valves and fuel injection). Manufacturer set the basic angle settings for the start of fuel injection and the opening of the exhaust valve, so different settings of these angles may worsen or improve the engine operating parameters.

Table 1 Specifications of selected marine diesel engine 6S50MC MAN B&W

Data description	Value
Process type	two-stroke, direct injection
Number of cylinders	6 in line
Cylinder bore	500 mm
Stroke	1910 mm
Ignition sequence	1-5-3-4-2-6
Maximum continuous rating (MCR)	8580 kW
Engine speed at MCR	127 min ⁻¹
Maximal mean effective pressure	18 bar
Maximal combustion pressure	143 bar
Specific fuel consumption (with high efficiency turbocharger)	171 g/kWh, on 100% load
Compression ratio (obtained by calculation)	17.2
Crank mechanism ratio	0.436
Exhaust manifold volume	6.13 m ³
Inlet manifold volume (with intercooler)	7.179 m ³

2.1 Engine available data from test bed

The main data of the marine diesel engine are obtained by measurement [8]. Such measurements are performed during the testing of the new engine on the test bed. Table 2 presents the measured values for the selected engine steady operation points at 25%, 50%,

75%, 93.5%, 100% and 110% of engine load. The engine was produced at the Shipyard Split under the MAN B&W license.

The examination was performed at the following environment state:

- Ambient temperature 30 °C,
- Ambient pressure 1005 mbar,
- Relative humidity 50%.

The engine was tested on diesel fuel D-2, whose features are, according to a supplier report:

- Density 844.7 kg/m³,
- Kinematic viscosity 3.03 mm²/s,
- Sulfur content 0.45%,
- Net caloric value 42.625 MJ/kg.

Table 2 6S50MC MAN B&W measured data [8]

Engine load (regarding MCR)	25%	50%	75%	93.5%	100%	110%
Indicated power (kW)	2401	4406	6580	8170	8656	9499
Effective power (kW)	2142	4099	6160	7667	8182	9014
Engine speed (min ⁻¹)	76.5	96	110.4	118.5	121.4	125.2
Controller Index	44.3	55.4	68.1	77.3	79.2	85.8
Compression pressure (bar)	46.2	70.3	97.5	117.6	123.7	137.8
Maximal combustion pressure (bar)	66.6	97.4	129.6	143.3	141.4	139.3
Mean indicated pressure (bar)	8.37	12.24	15.89	18.38	19.01	20.23
Fuel rack position (mm)	39.7	50.3	63.3	73	75	81.8
Intake manifold pressure (bar)	1.39	2.03	2.76	3.33	3.55	3.93
Intake manifold temperature (°C)	25	29	34	40	41	45
Exhaust manifold pressure (bar)	1.3	1.86	2.51	3.06	3.26	3.64
Temperature before turbine (°C)	308	327	346	384	404	458
Turbocharger rotational speed (min ⁻¹)	7290	11360	13870	15360	15895	17110
Specific fuel consumption (g/(kW·h))	186.83	174.06	171.18	171.82	174.66	180.5

2.2 Available data from simulation

The data and mathematical model, used in the simulations, are the results of scientific research project "Numerical simulation and optimization of marine diesel engines" (069-0691668-1725, Croatian Ministry of Science, Education and Sports). The developed MATLAB-SIMULINK simulation model gives satisfactory results, but unfortunately not sufficiently fast for engine real-time control and it is impractical for quick analysis. The accuracy provided by MATLAB-SIMULINK numerical simulations gave a relative error less than 3% in the interior and 5% on the borders of the engine operation field. This was a prerequisite for the high-quality neural network learning process in order to obtain her predictions at the same accuracy level. Numerical simulations can also investigate the engine working conditions outside the domain covered by the producer warranty. This is another reason why the developed MLP (Multilayer Perceptron) neural network used the results obtained by MATLAB-SIMULINK numerical simulations.

Original MATLAB-SIMULINK simulation [8] were performed by means of the engine controller acting to fuel rack regarding the load set by the propeller at engine constant speed. In the presented research, a set of engine data for randomly distributed operation points was

obtained by simulations. Before each simulation, input parameters were selected randomly. Simulations were stopped after convergence was reached. The convergence criterion was the convergence of air to fuel ratio in the cylinder. If this criterion was not met in 30 successively iterated engine cycles, convergence for that input point was not reached. For each simulation, a file of input and output data is kept. From that file, converged data points are selected and filtered. The filtering results in removal of data if the specific fuel consumption is outside the expected range (those points were not the real steady state points), Table 3.

Modern marine diesel engines with electro-hydraulic control of fuel injection and exhaust valve opening allow a very large area of engine customization in various modes. This entire area is usually too large for complete engine testing, and detailed measurements are not publicly available. This was precisely the reason due to which the development of the neural network was performed by using data obtained by numerical MATLAB-SIMULINK simulations.

Table 3 Simulated data from MATLAB-SIMULINK [8]

Engine load (regarding MCR)	25%	50%	75%	93.5%	100%	110%
Indicated power (kW)	2401.5	4407.5	6581	8169.5	8658.2	9499.7
Effective power (kW)	2141.7	4098.6	6159.7	7666.7	8181.8	9014
Engine speed (min ⁻¹)	76.5	96	110.4	118.5	121.4	125.2
Compression pressure (bar)	47	70.06	97	116.5	124.1	137.52
Maximal combustion pressure (bar)	69.9	94	126	144	142	140.1
Mean indicated pressure (bar)	8.37	12.24	15.89	18.383	19.01	20.23
Fuel rack position (mm)	39.23	50.83	63.73	72.37	75	81.9
Intake manifold pressure (bar)	1.38	2.075	2.83	3.36	3.554	3.925
Intake manifold temperature (°C)	23	26	33.55	39.15	40.95	44.5
Exhaust manifold pressure (bar)	1.3	1.89	2.58	3.05	3.24	3.6
Temperature before turbine (°C)	307	326	347	377	397	447
Turbocharger rotational speed (min ⁻¹)	7450	11356	13868	15360	15896	17113
Specific fuel consumption (g/(kW·h))	180	173.6	171.12	171.9	174.598	179.9

3. Neural network model

The power of the neural network is due to massively parallel distributed structure, and ability to learn, therefore to generalize. Generalization means that the neural network can produce "reasonable" outputs for inputs not seen during training or "learning", [9]. The smallest unit of an artificial neural network is the artificial neuron. The neuron makes the basic unit for processing the input to the output. The word artificially must be emphasized, because even though artificial neurons mimic biological neuron, it is different from biological and represents only its simplified model.

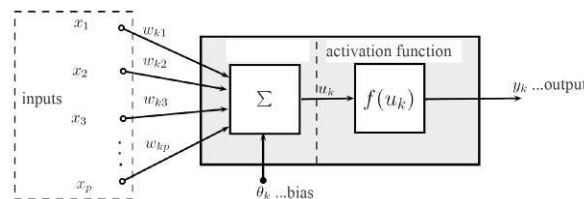


Fig. 1 Neuron with bias

Each artificial neuron has the following elements: inputs to neuron x_i , connection weights w_k , summation operator Σ , activation function f , bias θ_k and output from neuron y_k , Figure 1.

Linear sum of neuron inputs u_k is defined in following equation:

$$u_k = \sum_1^p w_{kj} - \theta_k \quad (1)$$

where w_{kj} are connection weights of k neuron with j input, and p is a number of neuron inputs. The output value from neuron y_k is defined in following equation:

$$y_k = f(u_k) \quad (2)$$

An MLP neural network with one hidden layer was chosen in this paper. The MLP neural network can have many hidden layers, Figure 2, but one layer is enough for output functions with continuous values.

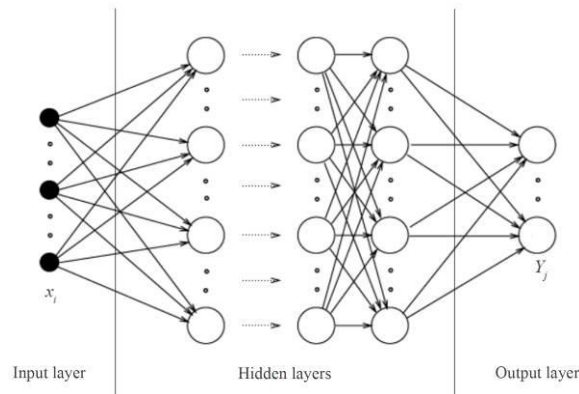


Fig. 2 MLP neural network

The hidden layer has a sigmoid function as activation function, one of the most used activation functions. The output layer also has a sigmoid function, although it is common to have a linear function in the output layer for the problems with continuous values in outputs. The linear function in the output layer was tried but for this problem a more stable convergence was achieved with the sigmoid function. Sigmoid function is defined as:

$$y(x) = \frac{1}{1 + e^{-x}} \quad (3)$$

The shape of training data dictates the number of neurons in the input layer and in the output layer. The number of neurons in the hidden layer has to be set. The strategy for finding number of hidden neurons was trying numbers in ascending order (2, 4, 10, 20, 40 and 80). The number of 40 neurons was chosen. Using more neurons would result in increased difficulties in finding weights without increasing the performance of neural network, FANN (Fast Artificial Neural Network) [10].

FANN library was used for neural network learning because of the performance it gives. Learning was achieved by a custom made application developed in C programming language. Post processing was performed in scripting programming language python with pyfann library (which uses the same FANN library).

Table 4 Input parameters range

Input parameter*	Value range**	Dimension
n_M	75 ... 130	min^{-1}
x_{reg}	12 ... 82.7	mm
SOI	-10 ... +10	$^{\circ}\text{CA}$
EVO	-20 ... +20	$^{\circ}\text{CA}$

* For details, see Input parameters in the Table 5

** regarding the reference value of the engine

Table 5 Input and output variables list

Ord.	Variable label	Variable description	Dimension
Convergence designation			
1	Konverg	Simulation convergence	1-Yes, 0-No
Input parameters			
2	n_M	Engine speed	min^{-1}
3	x_{reg}	Fuel rack position	mm
4	SOI	Start of injection	$^{\circ}\text{CA}$
5	EVO	Exhaust valve open	$^{\circ}\text{CA}$
Output values			
6	M_M	Engine torque	Nm
7	P_{ef}	Engine power	kW
8	b_e	Specific fuel consumption	g/kWh
9	T_{EM}	Exhaust manifold temperature	K
10	$T_{\text{out,T}}$	Turbine outlet temperature	K
11	T_{IM}	Intake manifold temperature	K
12	$m_{\text{flow,T}}$	Mass flow on the turbine	kg/s
13	λ_{EM}	Air excess ratio	-
14	p_{IM}	Intake manifold pressure	Pa
15	p_{EM}	Exhaust manifold pressure	Pa
16	n_{TC}	Turbocharger rotational speed	min^{-1}
17	$m_{\text{flow,C}}$	Mass flow on the compressor	kg/s
18	p_{max}	Maximum cylinder pressure	Pa
19	T_{max}	Maximum cylinder process temperature	K
20	Q_w	Heat transferred to the cylinder walls	J

The data available from simulation, organized as records, were divided into three data sets: for training, validation and testing. The training data set was used for training of network, validation data set was used to decide when to stop the training and testing data set for evaluation of the trained neural network performance. The size of the training data set is about 70% of data, and size of validation and testing data sets were 15% each. The lists of inputs and outputs with respective ranges and units are given in Table 4 and Table 5.

Input and output data were scaled in the range [0, 1]. Scaling is not mandatory for all MLP neural networks but the scaling of input data helps in finding initial weights giving all inputs of one record the equal importance.

Scaling of output values is important because of sigmoid activation function in output neurons. Data scaling can influence on training performance [11].

The MLP is a neural network that can be trained using supervised learning. In supervised learning, training data consist of input-output pairs, and the neural network is trying to find a mapping function that will generate the output for given input values. Through the learning process, the network changes their weights. In the training of the artificial neural network convergence depends on the initial start weights vector. So, to test some structure, it is necessary to repeat the process of learning with different randomly selected weights. Each parameter has influence on the performance. In this paper, a more advanced batch training algorithm iRPROP (improved resilient backpropagation) [12] was used, which is a variety of the standard RPROP (resilient backpropagation) training algorithm [13]. It achieves good results for many problems, the training algorithm is adaptive and the learning rate does not have to be specified.

The tanh error function is an error function that makes large deviations of stand-outs, by altering the error value used during the training of the network. This is the default error function in FANN. Usually it performs better, but, however it can give poor results with high learning rates, [10].

Table 6 Error level by number of data

	Training data (the number of data)					Validation data (the number of data)				
	<5%	<10%	<15%	≥15%	Σ	<5%	<10%	<15%	≥15%	Σ
M_M	783	23	3	0	809	190	10	0	0	200
b_e	809	0	0	0	809	200	0	0	0	200
T_{EM}	784	21	3	1	809	190	10	0	0	200
$T_{out,T}$	772	28	7	2	809	181	18	1	0	200
T_{IM}	785	22	2	0	809	196	4	0	0	200
$m_{flow,T}$	765	37	6	1	809	188	12	0	0	200
p_{IM}	803	6	0	0	809	200	0	0	0	200
p_{EM}	806	3	0	0	809	199	1	0	0	200
n_{TC}	797	11	0	1	809	199	1	0	0	200
$m_{flow,C}$	775	30	3	1	809	192	8	0	0	200
p_{max}	760	49	0	0	809	186	13	1	0	200
T_{max}	804	5	0	0	809	199	1	0	0	200

The learning of the neural network repeats from epoch to epoch by using the training algorithm. After each epoch the errors on training and on validation data are determined. The process of learning is repeated while errors are decreasing. Training with train data is stopped when the error on validation data set starts to increase. Usually the error values tend to oscillate so it is important not to stop the iterations immediately, but to try training for a number of epochs and keep the track of weights with the minimum error. Table 6 presents the errors of the most important output variables after achieving minimum error.

When displaying simulation results of the MLP neural network, it should be considered that the angle delay of the start of fuel injection (*SOI*) has a negative sign for earlier shift and positive sign for the later shift in regard to reference settings by the engine manufacturer. The same angle delay principle was used also for the exhaust valve opening (*EVO*).

4. The ANN model applications in engine operation optimization

After the neural network learning, some analyses have been carried out. The developed neural network model allows a fast calculation of the engine steady state operation parameters. In a very short time it is possible to cross the whole area of solutions for a given *SOI* and *EVO* and to calculate all the necessary characteristics [14]. The area solutions for searched *SOI* and *EVO* are available in discrete steps of 0.5 °CA. The decision making for the best *SOI* – *EVO* combination depends mostly on the specific fuel consumption b_e , the maximum cylinder pressure p_{max} and the maximum cylinder process temperature T_{max} [15], [16].

4.1 ANN results for a full engine load and for 50% engine load

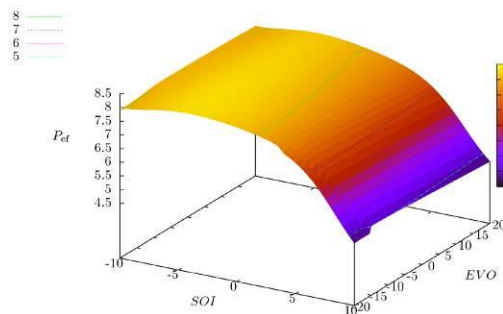


Fig. 3 Engine effective power, P_{ef} [MW]
- for a full load

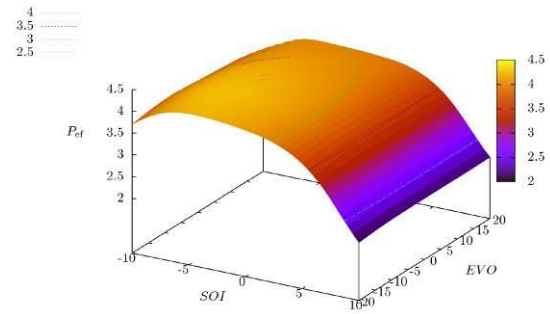


Fig. 4 Engine effective power, P_{ef} [MW]
- for a 50% load

Effective power shows the same trend, regardless of whether it is at full load or at 50% engine load, Figure 3 and Figure 4. *SOI* has a decisive influence on the engine effective power. The maximum effective power was reached with the start of fuel injection just before the engine factory settings. Moving the *SOI* for later reduces the effective power, and later injection causes the proportional decrease in effective power. *EVO* has an almost constant effect on the engine effective power for the selected *SOI*.

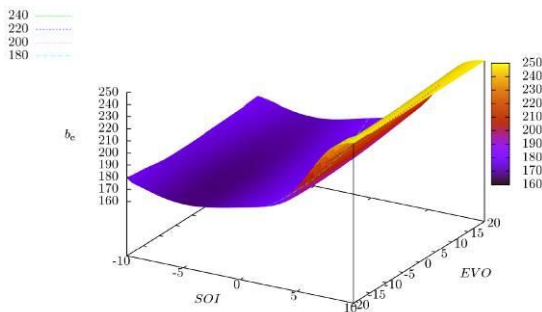


Fig. 5 Specific fuel consumption, b_e [g/kWh]
- for a full load

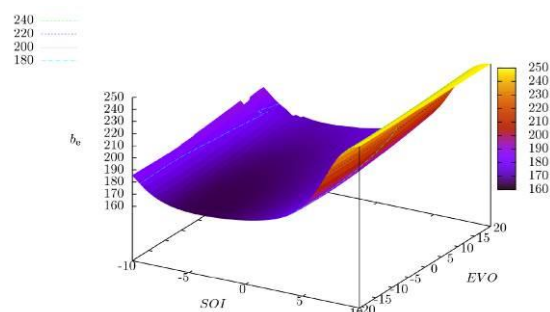


Fig. 6 Specific fuel consumption, b_e [g/kWh]
- for a 50% load

The specific fuel consumption has been the lowest for the *SOI* just before the factory settings, and the same is optimal for engine operation regarding the specific fuel consumption and effective power. Also in this situation, for specific fuel consumption, *EVO* has an almost

constant effect for the selected *SOI*. The specific fuel consumption change has a similar trend at full and at 50% engine loads, Figure 5 and Figure 6.

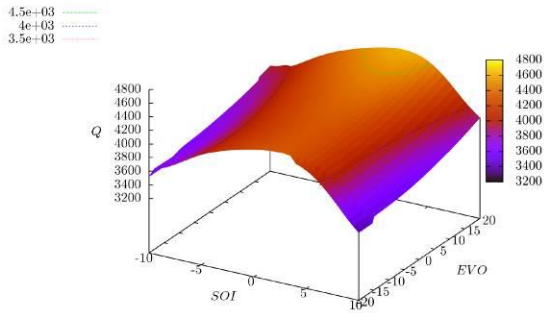


Fig. 7 Exhaust gases thermal flow at the turbine outlet, \dot{Q} [kW] - for a full load

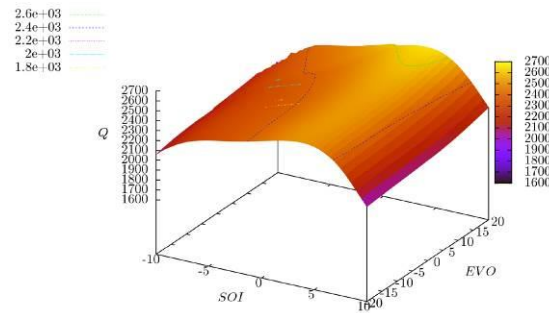


Fig. 8 Exhaust gases thermal flow at the turbine outlet, \dot{Q} [kW] - for a 50% load

The exhaust gases thermal flow at the turbine outlet leads to similar conclusions as for the exhaust gases temperature after the turbine, regardless of the engine load, Figure 7 and Figure 8. Although it is not explicitly visible in Figure 8, this picture also points to the engine operation instability at a very early *SOI* and late *EVO* at 50% load, which is reflected in the changes of the engine operation area borders.

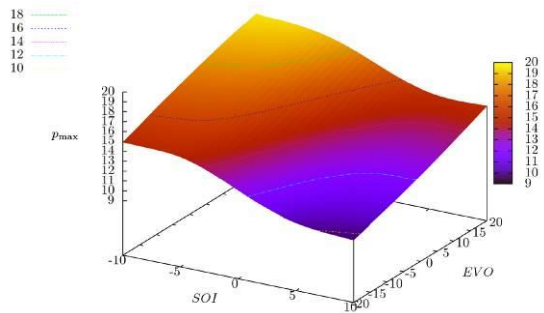


Fig. 9 Maximum pressure in the engine cylinder, p_{max} [MPa] - for a full load

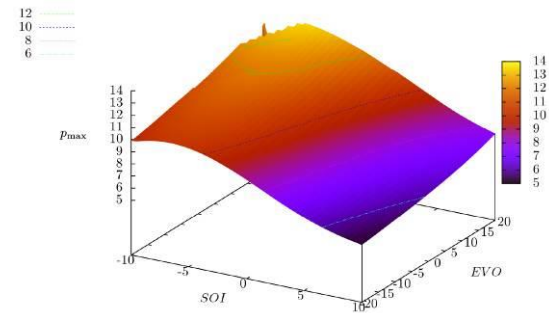


Fig. 10 Maximum pressure in the engine cylinder, p_{max} [MPa] - for a 50% load

At full engine load, Figure 9 shows that the maximum pressure in the cylinder is obtained for very early *SOI* shift and very late *EVO* shift. This working area at this engine load is stable and there is no danger of falling out of operation. Also, in this same area the effective power decreases and the specific fuel consumption increases, and surely this working area is not preferred for selection. The maximum cylinder pressure rapidly decreases for later *SOI* shift, and earlier *EVO* shift regarding to the engine referent values.

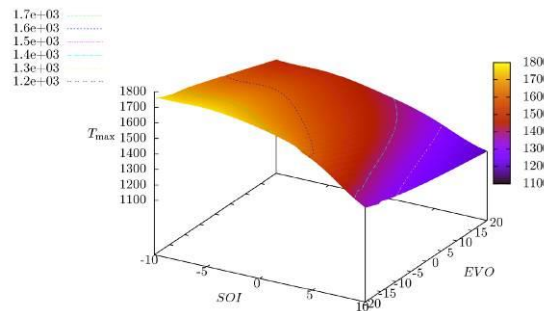


Fig. 11 Maximum temperature in the engine cylinder, T_{max} [°C] - for a full load

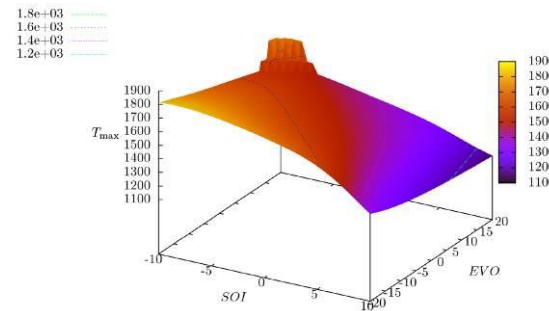


Fig. 12 Maximum temperature in the engine cylinder, T_{max} [°C] - for a 50% load

Maximum cylinder pressure at 50% load shows the same trend as for a full engine load, Figure 10. The only exception is the area of early *SOI* shift and late *EVO* shift, which also at this engine load shows unstable engine operation due to worsened scavenging process.

The highest temperature in the engine cylinder, for both of the observed loads was achieved at a very early *SOI* shift and proportionally early *EVO* shift, Figure 11 and Figure 12. However, it should be noted that too high temperatures in the engine cylinder cause high emissions, primarily emissions of nitrogen oxides, and under these conditions the engine certainly could not provide the required environmental standards. Regarding the maximum temperature of the engine process, usually a compromise between the achieved emissions and the produced heat necessary for utilization has to be found.

4.2 The optimization of *SOI* and *EVO* for maximum thermal flow of exhaust gases for utilization

The simulation results indicated that the *SOI* shift for 3.5 °CA later, and *EVO* shift for 20 °CA later, ensure the highest exhaust gas thermal flow, 9.5% higher than the reference one, Figure 13, with an increase in specific fuel consumption, Figure 14. The increase in specific fuel consumption is small enough, that increased fuel cost will be very quickly paid off by using higher obtained exhaust thermal flow for the utilization process. At the same time the engine power (ie. engine torque at the constant engine speed) decreased by approximately 7%, Figure 15.

Presented simulation results show justifiability for *SOI* and *EVO* shifts, in order to obtain a sufficient additional thermal flow, which can be effectively applied in the utilization process. In that way, it is possible to achieve significant savings in the ship propulsion plant with such a diesel engine and with the possibility of achieving multi-criteria optimization.

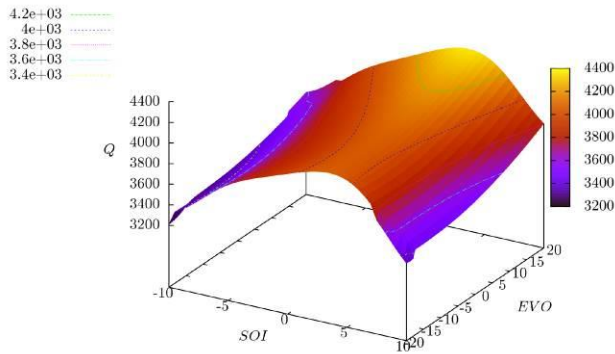


Fig. 13 Exhaust thermal flow \dot{Q} [kW] at the turbine outlet

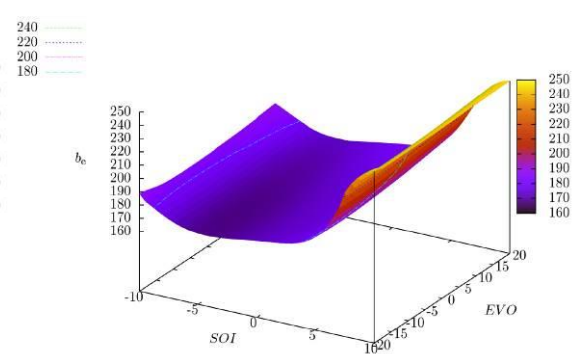


Fig. 14 Specific fuel consumption b_e [g/kWh]

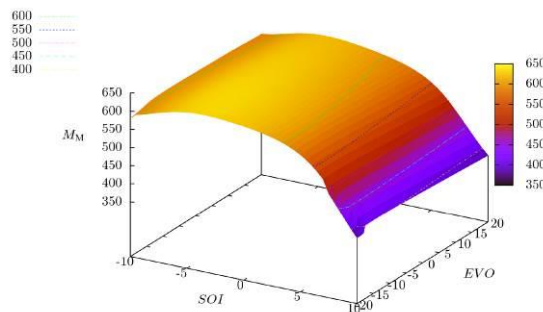


Fig. 15 Engine torque M_M [kNm]

In this mode of engine operation, excessive pressures and temperatures in the engine cylinder can be avoided, Figure 16 and Figure 17. This fact proves that the displayed change of operating parameters would not lead to significant thermal load increase, or to high increase in emissions. Such operating parameters change during the actual engine operation surely will result in a substantial impact on the entire propulsion plant efficiency.

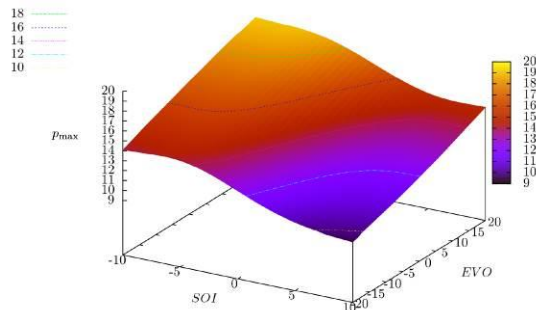


Fig. 16 Maximum pressure in the engine cylinder p_{max} [MPa]

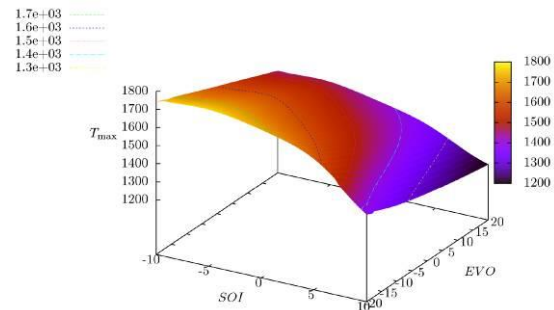


Fig. 17 Maximum temperature in the engine process T_{max} [°C]

Graphs in figures 5, 7, 9, 11 and figures 13, 14, 16, 17 are similar in shape but the ranges are not the same. The figures show various operating modes.

4.3 Satisfying the required thermal capacity at constant torque and engine speed

In this case, the engine operating point was given with engine speed $n_M = 118.5 \text{ min}^{-1}$ and the required torque $M_M = 465 \text{ kNm}$. The minimal required exhaust thermal flow after turbine $\dot{Q}_{min} = 3200 \text{ kW}$ was also given. The limits on the position of the fuel rack were between 40 and 75 mm. Additionally, the limits for the highest maximum temperature of the engine process $T_{max,lim} = 1900 \text{ °C}$ and the maximal allowable pressure in the cylinder $p_{max,lim} = 14 \text{ MPa}$ were also set. The pressure values from the simulation can exceed the limited value of 14 MPa but those working points are constrained in optimisation algorithm because they are not used in real engine operation.

The initial idea was to find the engine operation point at which all given conditions are met. For referent settings of *SOI* and *EVO* the given value of exhaust thermal flow was not achieved. In order to achieve the operating point where the parameters are equal or the nearest possible to default ones, *SOI* and *EVO* shifts were allowed.

In order to achieve and maintain the engine torque, since it varies by *SOI* and *EVO* shifts, it was necessary to make a fuel rack position correction. After this step, the engine has reached a working point where the desired thermal flow was satisfied. In that working point, the desired engine torque was also reached.

Simulation passes the entire field of *SOI* and *EVO* shifts, and for each of the shifts a new fuel rack position was calculated. With the new position of the fuel rack, the predefined engine torque and engine speed ($n_M = 118.5 \text{ min}^{-1}$, $M_M = 465 \text{ kNm}$) must be satisfied. Then it is checked if the new operation point satisfies a predetermined minimum exhaust thermal flow on the turbine outlet. Finally, the simulation checks if the newly determined operation point has a lower specific fuel consumption than the previous one. If at least one point satisfies all these conditions, the system has a solution.

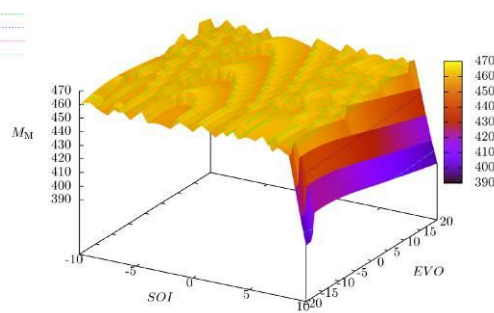


Fig. 18 Engine torque M_M [kNm]

At given operating conditions, engine torque shows almost constant value, but stable change for almost the entire working area, for all SOI and EVO shifts, Figure 18. The only exceptions are the areas of large SOI shift later than the reference value, with intense loss of engine torque, and thus engine power, due to the worsened scavenging conditions. A major SOI shift to later shows late fuel injection, so in this area incomplete combustion can be expected, which results in a huge loss of engine torque. It is necessary to avoid the area where these phenomena occur, because it is impossible to achieve a stable operating point.

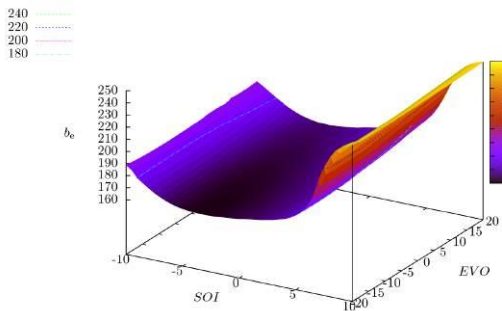


Fig. 19 Specific fuel consumption b_e [g/kWh]

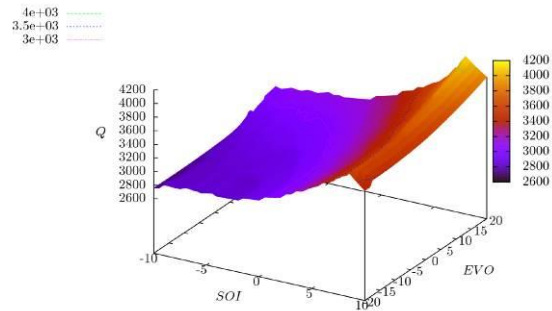


Fig. 20 Exhaust thermal flow \dot{Q} [kW]
at the turbine outlet

Even in this operation mode, specific fuel consumption was the lowest at the reference (factory) engine settings, Figure 19. Large increases in specific fuel consumption occurred only at intense shift of SOI for later, where a huge exhaust thermal flow at the turbine outlet was available, Figure 20, but it is necessary to avoid this operating area due to the large reduction in engine torque and highly probable fall-out from the drive, Figure 18. Maximum exhaust thermal flow, in the engine stable operation area, is presented in Table 7.

Table 7 Exhaust heat flow maximizing for a given $n_M = 118.5 \text{ min}^{-1}$ and $M_M = 465 \text{ kNm}$

SOI °CA	EVO °CA	M_M kNm	b_e g/kWh	x_{reg} mm	P_{ef} MW	T_{max} °C	p_{max} MPa	\dot{Q} kW
0	0	457.7	165.7	55	5.68	1452.2	11.67	2984.4
+4.5	-2.5	465	175.7	59	5.77	1404.6	10.28	3300.9

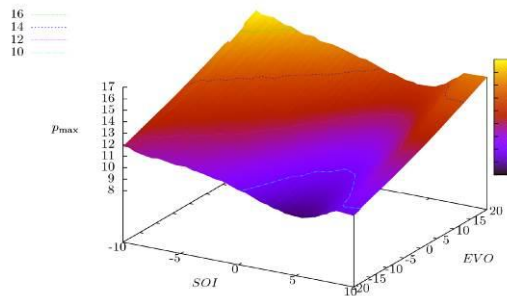


Fig. 21 Maximum pressure in the engine cylinder p_{max} [MPa]

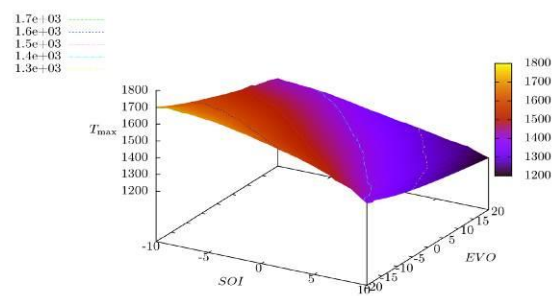


Fig. 22 Maximum temperature in the engine process T_{max} [$^{\circ}C$]

Maximum cylinder pressure occurs in areas of very early *SOI* shift, and very late *EVO* shift, Figure 21. Therefore, for the maximum cylinder pressure it is optimal to hold *SOI* and *EVO* parameters to reference values, with the recommended *EVO* shift to earlier, in order to avoid excessively high pressures. In this area, other operating parameters do not indicate a sudden or unexpected change, so this engine operating area would be advisable for given conditions. *EVO* shift to earlier, while retaining the referent *SOI*, would be recommended also for maximum engine process temperature, Figure 22, because the maximal temperature would be optimal for utilization, and thermal load of engine working parts or emissions remain acceptable. The optimal solution could be achieved also with more complex methods of optimization (multi-criteria optimization, multi-objective optimization, etc.).

5. Conclusion

In this paper, the changes in the characteristics of "intelligent" marine two-stroke diesel engine were studied, when crank angles for the start of fuel injection (*SOI*) and for the opening of the exhaust valve (*EVO*) were shifted. The fuel injection strategy (fuel injection flow) and the exhaust valve opening curve did not change, which was left for future research. The investigations have pointed to the great potential that provides electro-hydraulic control of fuel injection and exhaust valve drive to bring the modern marine diesel engine in the desired working conditions.

Some examples of the described neural network applications in optimization of marine diesel engine were presented, in order to achieve the desired exhaust heat flow for the utilization purposes, along with minimum specific fuel consumption, as well as to maintain maximum engine process temperature as low as possible in order to reduce NO_x emission.

The developed neural network model is fully prepared for the reception of new data, measured during the engine operation. With comparisons of measured data and data obtained by the neural network, it will be possible to evaluate the quality of measured data and the entire measuring system. This was already proven on various sets of measured data.

The neural network model was developed using data obtained from numerical simulations, for the engine steady state operation, with verification from available data measured on the test bed. Therefore, the existence of high-quality numerical simulation model in neural network development was very important. Also, the resulting neural network model has limitations (eg. the model is valid for engine steady state operation, for the same type of engine, the same selected turbocharger etc., but the obtained structure can effectively learn on the data for a new engine type).

Data for the neural network learning and testing must be within all steady state regimes of engine operation. But once the requested data were obtained, and neural network optimized, learned and operational, it is capable to give the required engine data almost 3000 times faster in regards to conventional numerical simulation.

REFERENCES

- [1] Blair, G. P.: *Design and simulation of two-stroke engines*, SAE Publishing, Warrendale, ISBN-13: 978-1560916857, 1996.
- [2] Medica, V.: *Simulation of turbocharged diesel engine driving electrical generator under dynamic working conditions*, Doctoral Thesis, University of Rijeka, Rijeka, 1988.
- [3] Arcaklioğlu, E., İsmet Çelikten.: *A diesel engine's performance and exhaust emissions*, Applied Energy, 80:11–22, 2005.
- [4] He, Y., Lin, C. C.: *Development and validation of a mean value engine model for integrated engine and control system simulation*, SAE Paper 2007-01-1304, 2007.
- [5] Mrakovčić, T.: *Osnivanje i vođenje brodskog pogonskog postrojenja primjenom numeričke simulacije (Design and control of marine propulsion plant using numerical simulation, in croatian)*, Doctoral Thesis, University of Rijeka, Rijeka, 2003.
- [6] Brahma, I., Rutland, C. J.: *Optimization of diesel engine operating parameters using neural networks*, SAE Journal of Fuels and Lubricants, Vol. 112, No. 4, pp. 2521-2529, 2004.
- [7] He, Y., Rutland, C. J.: *Modeling of a turbocharged di diesel engine using artificial neural networks*, SAE Paper 2002-01-2772, 2002.
- [8] Račić, N.: *Simulacija rada brodskog propulzijskog sustava sa sporohodnim dizelskim motorom u otežanim uvjetima (Simulation of performance of the ship propulsion system with slow speed diesel engine in aggravated conditions, in croatian)*, Doctoral Thesis, University of Rijeka, Rijeka, 2008.
- [9] Haykin, S.: *Neural Networks - a Comprehensive Foundation*, Macmillan, New York, 1994.
- [10] <http://leenissen.dk/fann/wp/> (last visited 08.09.2015.)
- [11] Koprinkova, P., Petrova, M.: *Data-scaling problems in neural-network training*, Engineering Applications of Artificial Intelligence, 12:281–296, 1999.
- [12] Igel, C., Hüsken, M.: *Improving the Rprop Learning Algorithm*, Second International Symposium on Neural Computation (NC 2000), pp. 115-121, ICSC Academic Press, 2000.
- [13] Riedmiller, M.: *Rprop - Description and Implementation Details*, Technical Report, University of Karlsruhe, 1994.
- [14] Bukovac, O.: *Predviđanje parametara rada brodskog dizelskog motora primjenom neuronskih mreža (Prediction of marine diesel engine's operating parameters using neural networks, in croatian)*, Doctoral Thesis, University of Rijeka, Rijeka, 2012.
- [15] Deng, J., Maass, B., Stobart, R.: *Using artificial neural networks for representing the brake specific-fuel consumption and intake manifold pressure of a diesel engine*, Power and Energy Engineering Conference, APPEEC 2009, Asia-Pacific, 2009.
- [16] Parlak, A., Islamoglu, Y., Yasar, H., Egrisogut, A.: *Application of artificial neural network to predict specific fuel consumption and exhaust temperature for a diesel engine*, Applied Thermal Engineering, 26:824–828, 2006.

Submitted: 04.11.2015.

Accepted: 21.12.2015.

Ozren Bukovac, Vladimir Medica, Vedran Mrzljak, vmrzljak@riteh.hr
Faculty of Engineering, University of Rijeka
Vukovarska 58, 51000 Rijeka